Wettability Alteration and Enhanced Oil Recovery Induced by Proximal Adsorption of Na^{+}, Cl^{−}, Ca^{2+}, Mg^{2+}, and SO_{4}^{2−} Ions on Calcite

Jian Liu, Omar B. Wani, Saeed M. Alhassan, and Sokrates T. Pantelides

Phys. Rev. Applied **10**, 034064 — Published 27 September 2018

DOI: 10.1103/PhysRevApplied.10.034064

Wettability alteration and enhanced oil recovery induced by proximal adsorption of Na^+, Cl^-, Ca^{2+}, Mg^{2+}, and SO_4^{2-} ions on calcite

Jian Liu[1,*] Omar B. Wani[2], Saeed M. Alhassan[2], and Sokrates T. Pantelides[1,3]

[1]Department of Physics and Astronomy, Vanderbilt University, Nashville, Tennessee 37235, USA

[2]Department of Chemical Engineering, Khalifa University of Science and Technology, Abu Dhabi, UAE

[3]Department of Electrical Engineering and Computer Science, Vanderbilt University, Nashville, Tennessee 37235, USA

The underlying wettability alteration mechanism responsible for enhanced oil recovery (EOR) in carbonate reservoir is a long-standing issue for which no consensus has been reached yet. In this paper, we report extensive quantum molecular dynamics simulations to reveal the roles of wettability modifiers Na^+, Cl^-, Ca^{2+}, Mg^{2+}, and SO_4^{2-} ions in EOR. Characterizing wettability by contact angle using the work-of-adhesion approach, we find that the calcite surface is strongly hydrophilic, with the first two wetting layers hindering all ions from reaching the surface, i.e. ions are only "proximally adsorbed". Na^+ and Cl^- ions settle closer to the surface and actually disturb the interfacial water structure of the first two wetting layers, which renders the surface *less* water-wet and thus inhibits oil recovery, as observed. Ca^{2+}, Mg^{2+} and SO_4^{2-} ions, on the other hand, settle farther from the surface and retain the interfacial water structure, but render the surface *more* water-wet by modifying the effective charge on the surface, which enhances oil recovery, as observed. The impact of the ions is more pronounced at high temperatures as proximal adsorption is enhanced. In addition to theory, we report new core flooding measurements that corroborate the theoretical results. The present study brings new insights into the wettability alteration mechanism in EOR at the atomic scale.

Corresponding Author

[*]Email: Jian.Liu@alumni.stonybrook.edu.

I. INTRODUCTION

Surface wettability impacts a variety of issues that pertain to applications[1-4]. One of the major challenges in the oil industry is the enhancement of oil recovery (EOR) by water flooding in carbonate reservoirs[5-17]. Injection of smart water (water with optimized composition and salinity) is an efficient way of achieving EOR and wettability alteration has been proposed to be the driving mechanism[6]. Despite its importance, there exists no consensus on the specific wettability alteration mechanism that causes EOR[8]. A satisfactory understanding of wettability alteration has been lacking, due to the complicated interplay between ions such as Ca^{2+}, Mg^{2+}, SO_4^{2-}, Na^+ and Cl^- in saline water and the calcite ($CaCO_3$) surface.

Many experimental studies have been performed in an attempt to unveil the underlying mechanism behind wettability alteration. It was found by zeta-potential measurements that Ca^{2+}, Mg^{2+} and SO_4^{2-} are strong potential-determining ions (ions that are strongly related to the surface charge/potential), while SO_4^{2-} must act together with either Ca^{2+} or Mg^{2+} in order to improve the oil recovery[9-13]. Raising the temperature has been found to be of great benefit for EOR[12,14], while at high temperatures Mg^{2+} can even substitute Ca^{2+} from the chalk surface[12]. More recently, the injection of low-salinity brine in carbonate reservoirs was reported to enhance oil recovery[14-16,18-20]. It was further demonstrated that the low-salinity effect results from wettability alteration rather than mineral dissolution[19,21], but the specific mechanism responsible for the wettability alteration remains largely unknown.

On the theoretical side, atomic-scale simulations of wettability has usually been based on classical molecular dynamics (MD) using model potentials, focusing mainly on the competitive adsorption of organic molecules in water[22-27]. It has been challenging to investigate wettability alteration mechanism by classical MD, possibly due to fundamental difficulties in the construction of complicated model potential, particularly when many parameters are involved so as to properly describe the interactions between water, the calcite surface and the solvated ions. For example, contradictory results have been obtained on the preferential adsorption positions of Na^+ and Cl^- ions[28-31] using classical MD simulations.

Density functional theory (DFT) is the method of choice for parameter-free, quantum-mechanical characterization of the complex interplay at the calcite/brine/oil interfaces. Previous DFT calculations[32-37] studied the ion substitution mechanism[12], using the microscopic binding energies of water molecules and model organic compounds on calcite surfaces as the wettability indicator, treating the water at various levels of approximation. The true indicator of wettability alteration, however, is the macroscopic contact angle, which captures the adhesion properties of the liquid to the solid surface. This point is especially important when one is considering the effect of additive ions in the liquid. More recently, first-principles quantum MD simulations of such a solid-liquid interface were performed to study the intrinsic water wettability of the calcite surface[38], without considering the effect of brine composition and salinity.

In this paper, we report extensive quantum MD simulations to elucidate the underlying mechanism responsible for wettability alteration of the calcite surface by the injection of ions in the water. We use quantum MD simulations to extract the work of adhesion of pure water and water containing select ions, which allows us to calculate the corresponding contact angles. We find that the calcite surface is strongly hydrophilic. The first two wetting layers hinder all ions from reaching the surface, i.e. ions are only proximally adsorbed. The proximal adsorption of Na^+, Cl^- and Ca^{2+}, Mg^{2+}, SO_4^{2-} ions affects the wettability in different ways: the former settle closer to the surface and actually disturb the interfacial water structure of the first two wetting layers, *reducing* the contact angle and thus rendering the calcite surface less water-wet, which inhibits oil recovery, while the latter settle farther from the surface and retain the interfacial water structure, but *increase* the contact angle and thus render the surface more water-wet by modifying the effective charge on the calcite surface, which enhances oil recovery. The role of these ions as wettability modifiers is more pronounced at high temperatures, as the proximal adsorption is enhanced. All results from our quantum MD simulations are in line with experimental observations. We also report new core-flooding measurements for smart water that further corroborate the theoretical results. We find that injection of diluted seawater with the addition of sulfates significantly enhances oil recovery, in line with the theoretical findings. We also find that further removal of calcium ions has negligible impact. The present study provides physical insights into the role of wettability modifiers (Na^+, Cl^- and Ca^{2+}, Mg^{2+}, SO_4^{2-} ions), unraveling at the atomic scale the wettability alteration mechanism responsible for EOR.

II. THEORY AND METHODS

A. Theory. The wettability of a surface is characterized by the contact angle, a macroscopic quantity that is easily accessible in experiments, as opposed to the relative microscopic adsorption energies of molecules. Indeed, the significance of the binding energy as the wettability indicator has been questioned by results of classical MD simulations that predict similar binding energies but yield different contact angles[39]. In the present study, we use the contact angle as a reliable indicator for wettability alteration. One can extract the contact angle from the sessile droplet configuration of the calcite/brine/oil system. This method is particularly reliable using classical MD when one can use fairly large droplets. Here we use the work-of-adhesion approach[39-43], which we used successfully to investigate the water wettability of graphene[44] and hexagonal boron nitride[45] monolayers at the electronic structure level. We first give a brief description of the approach.

Starting with the Young-Dupré equation[46], the interfacial tensions γ of three two-phase interfaces (S-solid; L-liquid; O-oil; V-vapor) are related by

$$\gamma_{\mathrm{SL}} - \gamma_{\mathrm{SO}} = \gamma_{\mathrm{OL}} \cos\theta, \tag{1}$$

where θ is the oil-in-brine contact angle (see the schematic diagram in Fig. 1a). Noting that γ in the Young-Dupré equation is the free energy per unit area when an interface is created[47], the work of adhesion W_{adh} is related to the surface tensions γ by

$$W_{\mathrm{adh}}^{\mathrm{SL}} = \gamma_{\mathrm{SV}} + \gamma_{\mathrm{LV}} - \gamma_{\mathrm{SL}}. \quad (2)$$

In pioneering studies with the work-of-adhesion approach, one first computes the work of adhesion of a water slab on a surface and then employs the Young-Dupré equation that relates the work of adhesion to the water contact angle (WCA) θ_{WCA}[39-43]:

$$W_{\mathrm{adh}}^{\mathrm{SL}} = \gamma_{\mathrm{LV}}(1 + \cos\theta_{\mathrm{WCA}}), \quad (3)$$

where γ_{LV} is the surface tension of water (72.0 mJ/m^2)[48]. In terms of the work of adhesion, the wettability of the calcite/brine/oil system is determined by the competition in W_{adh} between the two interfaces (SL and SO)

$$W_{\mathrm{adh}}^{\mathrm{SO}} - W_{\mathrm{adh}}^{\mathrm{SL}} = \gamma_{\mathrm{OL}}\cos\theta - \gamma_{\mathrm{LV}} + \gamma_{\mathrm{OV}}. \quad (4)$$

In such competition, the water-wet conditions ($W_{\mathrm{adh}}^{\mathrm{SL}} > W_{\mathrm{adh}}^{\mathrm{SO}}$) are signified by larger θ, whereas the oil-wet conditions ($W_{\mathrm{adh}}^{\mathrm{SO}} > W_{\mathrm{adh}}^{\mathrm{SL}}$) are signified by smaller θ, as manifested in Eq. (4) where γ_{LV}, γ_{OV}, and γ_{OL} are nearly constants.

It has been believed that the carbonate reservoir is initially oil-wet due to the adsorption of polar carboxylic end groups that are present in crude oil[12]. MD simulations confirmed that alcohols with molecular mass greater than that of methanol could displace water at the calcite surface[49,50]. Also, recent experiments showed that organic acids adsorb directly onto the calcite surface[51]. In the oil-wet initial state, since oil contacts the calcite surface, ions solvated in brine do not necessarily contact the oil phase (see the schematic diagram in Fig. 1a). It is then clear that ions as wettability modifiers modify only the water wetness ($W_{\mathrm{adh}}^{\mathrm{SL}}$) but not the oil wetness ($W_{\mathrm{adh}}^{\mathrm{SO}}$) of the calcite surface. Varying brine composition and salinity then results in wettability alteration, the magnitude of which is characterized by

$$-\Delta W_{\mathrm{adh}}^{\mathrm{SL}} = \gamma_{\mathrm{OL}}\Delta\cos\theta. \quad (5)$$

It is also clear from Equations (4) and (5) that, the oil-wetness of the calcite surface affects wettability alteration only through setting an initial wetting state θ_0. In many cases, θ_0 varies with the experimental conditions such as the model oil used representing crude oil. To quantify $\Delta\theta$ without loss of generality, following Ref. [32], we assume the initial state to be mixed-wet ($\theta_0 \sim 90°$).

Exact evaluation of $W_{\mathrm{adh}}^{\mathrm{SL}}$ with quantum MD simulations is currently impractical due to the excessive computational cost in calculating the entropy, while relatively good values can be obtained for the internal energy. Nevertheless, it has been demonstrated by classical MD simulations that the entropic contribution to $W_{\mathrm{adh}}^{\mathrm{SL}}$ is roughly a third of the enthalpic contribution (energy of adhesion, $E_{\mathrm{adh}}^{\mathrm{SL}}$)[40,52]. We, therefore, approximate $W_{\mathrm{adh}}^{\mathrm{SL}}$ with $E_{\mathrm{adh}}^{\mathrm{SL}}$, where $E_{\mathrm{adh}}^{\mathrm{SL}}$ is obtained via quantum MD simulations. This choice has been demonstrated to suffice for the water wettability of graphene[44] and hexagonal boron nitride[45] monolayers at the electronic structure level. It represents a trade-off with sufficient accuracy to characterize wettability at the

atomic scale and allows for the interplay at the interfaces of calcite/brine/oil to be treated explicitly by quantum mechanics.

B. Computational details. Electronic structure calculations are performed in the basis of linear combinations of localized atomic orbitals, as implemented in the SIESTA package[53]. A variationally optimized double-ζ polarized (DZP) basis set is used with a mesh cutoff of 250 Ry for the real-space grid. After structural relaxations through total-energy and force calculations, DFT-based QMD simulations are performed. In order to correctly describe the density and diffusivity of liquid water at room temperature (with the PBE functional)[54-56], an elevated temperature of 360 K is maintained by the Nosé-Hoover thermostat. For each MD simulation, a trajectory of 2 ps is used for production after an equilibration stage of 3 ps, with a time step of 0.5 fs. The effect of temperature is investigated in a less rigorous manner. The initial positions and velocities of the simulation at 420 K are generated from the final snapshot of the simulation at 360 K, with only 1 ps used for production after an equilibration stage of 1 ps. To evaluate the interfacial energy, in the production stage, snapshots are taken every 20 fs. Ghost orbitals[57] are introduced to correct for the basis set superposition error wherever necessary.

The calcite $(10\bar{1}4)$ surface is represented by four layers of $CaCO_3$ units with 16.67×15.40 Å^2 surface area (in total of 240 atoms). The bottom two layers are held fixed at their equilibrium positions, while the top two layers are allowed to equilibrate. The formation water contains a relatively high concentration of Na^+ (~ 1.7 M), Cl^- (~ 3.3 M), and Ca^{2+} (~ 0.3 M), compared to seawater (~ 0.6 M for Na^+, ~ 1.1 M for Cl^-, and ~ 0.02 M for Ca^{2+})[8]. In each case studied, brine is modeled by 168 water molecules (pre-equilibrated in a cubic box), with one pair of ions (Ca^{2+}, Mg^{2+}, Na^+) and counter-ions (SO_4^{2-}, Cl^-) added accordingly which corresponds roughly to 0.3 M concentration, except for NaCl brine where two pairs of ions are added to mimic seawater. We adopt the Mulliken population analysis[58] to reveal the correlation between wettability and the surface charge, the latter of which is obtained from $\sum_{\mathrm{surface}}(\mathrm{Q_{atom}} - \mathrm{Q_{Mulliken}})$.

The weak dependence of the surface tension of water γ_{LV} on brine composition and salinity[59] has been neglected. Throughout the present study, the experimentally measured interfacial tension of alkane/water (51.7 mJ/m^2)[60] is adopted to represent γ_{OL}. For the composition and salinity covered in this study, the variation in the interfacial tension of brine/hydrocarbon system[61,62] is less than 2 mJ/m^2.

C. Experimental procedures

Carbonate outcrop cores used in the experiments were obtained from Kocurek Industries, USA. The petrophysical properties of the cores are summarized in Table 1. Core #1 was used for core flooding experiment whereas core #2 and #3 were used for spontaneous imbibition experiments. Synthetic brines were prepared by adding desired salts in de-ionized water. The prepared brines were filtered through 0.45 μm filter papers to remove any suspended particles. The compositions of the synthetic brines are presented in Table 2. All the cores were vacuumed initially for 4 hours before being imbibed by formation brine at a pressure of 2500 psi for 60 hours. Core #1 was

saturated with NaCl brine having the same ionic strength as that of ADNOC's formation brine, whereas cores 2 and 3 were saturated with ADNOC formation brine. Crude oil was injected into core #1 to displace the formation brine. The crude oil was injected until no more formation brine was produced and the core flooding system achieved a steady state in terms of delta pressure. Core #2 and #3 were put in special centrifuge tubes and soaked in crude oil for formation water displacement using a high-speed ultra-centrifuge at speeds from 1000 rpm to 12000 rpm for 150 hours. The centrifuge speed was increased every 30 hours. The cores were aged for 2 weeks in the same crude oil to allow wettability alteration and thereby obtain strongly oil-wet surfaces. Core #1 was aged at 120°C whereas core #2 and #3 were aged at 90°C. The dead ADNOC crude oil used in the experiments had a density of 0.836 g/cm^3 and viscosity of 5.34 cP at a temperature of 20 °C. The oil was filtered through 0.45 μm filter paper to remove impurities.

After oil ageing, core #1 was loaded into the core flooding system again and injected with crude oil to calculate the final saturation. The recovery studies were then started by injecting formation brine at a flow rate of 0.2 cc/min, the flow rate was then changed to 1 cc/min for nearly 2 pore volumes of injection, after this the injection flow rate was reduced to 0.01 cc/min for a shut-in period. Since wettability alteration is a very slow process and sufficient time should be given for the interaction between crude oil brine and rock, we introduce the shut-in period during the injection of each brine. The system remained in shut-in period for 10 pore volumes during formation brine injection. After the first shut-in period, the flow rate was increased to 1 cc/min for 1 pore volume of injection before switching to 4dSW. The same injection strategy was followed for 4dSW and 4dSW3S. The core flooding experiments were performed at a temperature of 120°C, confining pressure of 500 psi and a back pressure of 150 psi. Core #2 and #3 were placed in dry Amott imbibition cells after oil ageing. The cells containing core #2 and #3 were filled with 4dSW3S and 4dSW3S0Ca respectively. The imbibition cells were placed in an oven kept at a temperature of 70 °C. The oil recovery was noted on a daily basis through the graduated part of the Amott cells. The ionic strength of all the smart brines used in the experiments were kept constant to 0.164M and were pre-equilibrated with crushed core powder prior to the use.

Table 1 Petrophysical properties of the cores.

Core #	Length (cm)	Diameter (cm)	Porosity (%)	Permeability (mD)	Pore volume (cm^3)
1	7.0	3.8	16.2	35	12.9
2	3.4	3.8	15.4	32	5.8
3	3.3	3.8	16.5	42	6.2

Table 2 Compositions (in unit of M) of synthetic brines.

Ions	FW	4dSW	4dSW3S	4dSW3S0Ca	NaCl
Na^+	3.120	0.115	0.103	0.112	5.0
Ca^{2+}	0.526	0.003	0.003	0	0
Mg^{2+}	0.126	0.011	0.011	0.011	0

Cl^-	4.424	0.131	0.095	0.098	5.0
HCO_3^-	0	0.001	0.001	0.001	0
SO_4^{2-}	0	0.006	0.018	0.018	0
Ionic strength	5.0	0.164	0.164	0.164	5.0

III. RESULTS

Extensive quantum MD simulations have been performed to investigate the intrinsic water wettability of the calcite surface and the roles of wettability modifiers Na^+, Cl^-, Ca^{2+}, Mg^{2+}, and SO_4^{2-} ions in wettability alteration. The simulation supercell is schematically shown in Fig. 1b. The main results are summarized in Fig. 1c. We will discuss these results and related issues in detail below.

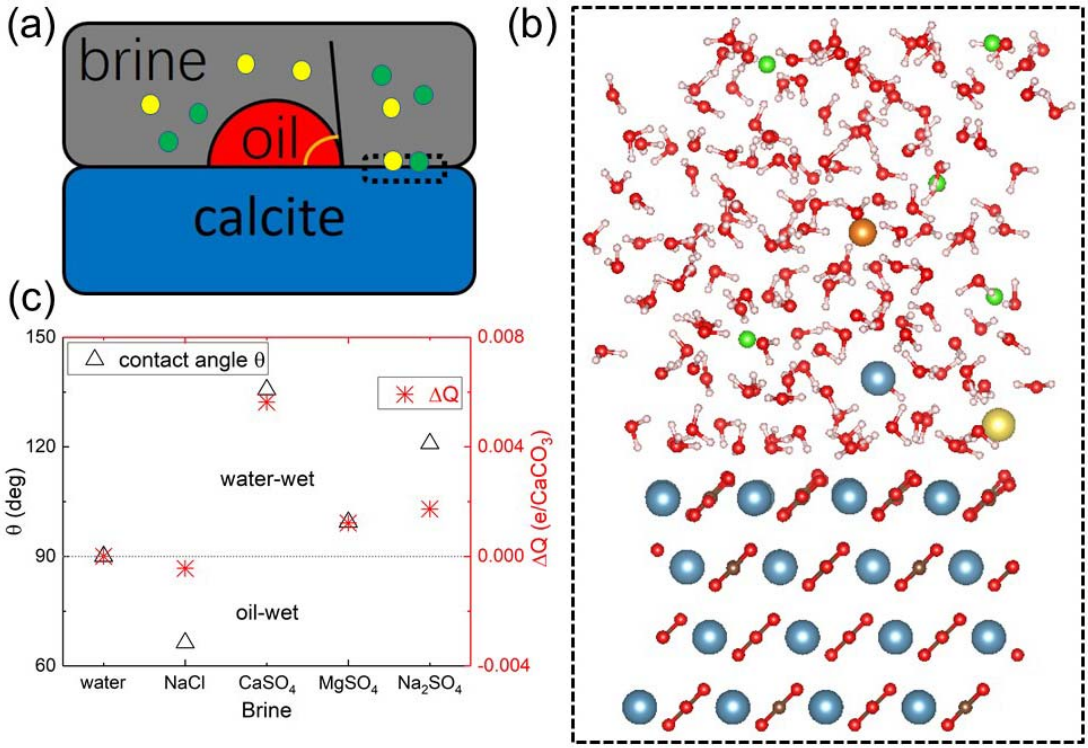

Figure 1. (a) Schematic diagrams of the calcite/brine/oil system. (b) Simulation supercell (color scheme: Ca-indigo, C-brown, O-red, H-white). Ions in brine are only shown schematically. (c) Left *y*-axis: oil-in-water contact angle assuming an initial mixed-wet state; Right *y*-axis: difference (relative to calcite-water) in the effective charge of the surface (estimated from Mulliken population analysis, in units of electron per surface $CaCO_3$ unit).

A. Intrinsic water wettability of the calcite surface

We start our discussion by investigating the intrinsic water wettability of the calcite surface. The density profile of water molecules near the surface is considered to have direct relevance on the

wettability, i.e. water molecules are closer to a more hydrophilic surface as a result of stronger adsorption. As shown in Fig. 2a, two peaks are found for the first and second water layers at 2.4 and 3.2 Å respectively, in agreement with previous theoretical and experimental results[63,64]. Graphene is considered to be weakly hydrophilic with a WCA slightly lower than 90°. Compared to the first two wetting layers at around 3.1 and 5.6 Å for graphene[44], the calcite surface is strongly hydrophilic (we will discuss the WCA of calcite shortly).

The strong hydrophilicity of the calcite surface is also manifested in the orientation angle (φ, defined as the angle between the H-O-H bisecting vector and the surface normal) distribution of water molecules in the first two wetting layers, as shown in Fig. 2b. According to the Fowkes approach[65,66], W_{adh} can be divided into a polar (electrostatic such as hydrogen bonding) part and a nonpolar (dispersive or van der Waals) part. For a nonpolar surface such as graphene, W_{adh} arises solely from dispersive interactions[44]. Indeed, for graphene water molecules in the first wetting layer preferably have their dipole moments pointing parallel to the surface ($\varphi \sim 90°$). For the calcite surface, we find that $\varphi \sim 60°$, i.e. polar interaction is invoked, resulting in strong water adsorption.

A closer examination reveals the detailed structure of interfacial water molecules, as shown in Fig. 2c for the O-H bond angle (α, defined as the angle between the O-H bond vector and the surface normal) distribution. Water molecules in the first wetting layer are bonded to surface Ca^{2+} ions, while water molecules in the second wetting layer tend to have their O-H bonds pointing to the topmost protruding O^{2-} ions in the surface CO_3^{2-} group. Such interfacial water structure originates from the hydrogen-bonding network at the interface, as highlighted in Fig. 2d. Furthermore, from the planar-averaged charge density difference $\langle \rho_{\mathrm{calcite-water}}(z) - \rho_{\mathrm{calcite}}(z) - \rho_{\mathrm{water}}(z) \rangle$, we find that electrons are transferred from the calcite surface to the interfacial water. Therefore, the calcite surface exhibits strong hydrophilicity, due to the electrostatic interaction that results from electronic redistribution.

The question then arises: What is the WCA of the calcite surface? To answer this question, we have calculated $E_{\mathrm{adh}}^{\mathrm{SL}}$ and found it to be 527 mJ/m^2. Taking approximately into account the entropic contribution (for graphitic carbon surfaces, a constant 33% of the enthalpic contribution, regardless of the number of graphene layers[40]), $W_{\mathrm{adh}}^{\mathrm{SL}}$ is 353 mJ/m^2, significantly larger than the surface tension of water γ_{LV} (72.0 mJ/m^2)[48]. From Eq. (3), such large $W_{\mathrm{adh}}^{\mathrm{SL}}$ indicates that water completely wets the calcite surface, as found in WCA measurements on freshly cleaved calcite surface[67]. It has also been shown by classical MD simulations that water completely wets the calcite surface in the dodecane phase[27]. Note, however, that from Eq. (4), for the competitive wetting of oil and brine on the calcite surface, a finite oil-in-brine contact angle is possible if $W_{\mathrm{adh}}^{\mathrm{SO}}$ is comparable to $W_{\mathrm{adh}}^{\mathrm{SL}}$.

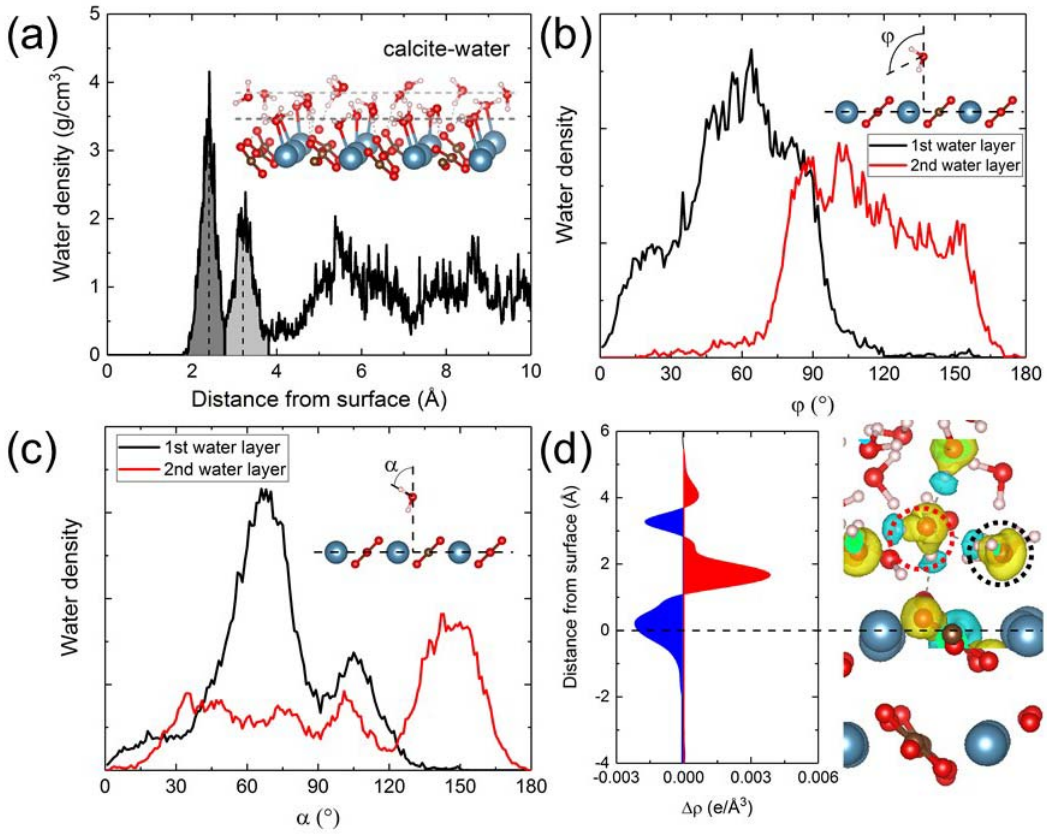

Figure 2. (a) Water density profile along the surface normal. Dashed lines indicate the positions of the first two wetting layers at 2.4 and 3.2 Å respectively (marked also by shaded areas). (b, c) Orientation angle and O-H bond angle distributions of water molecules in the first and second wetting layers. (d) Left: (ensemble-averaged) planar-averaged charge density difference $\langle \rho_{\mathrm{calcite-water}}(z) - \rho_{\mathrm{calcite}}(z) - \rho_{\mathrm{water}}(z) \rangle$. Red and blue shaded areas denote for electrons accumulation and depletion respectively. Right: isosurface of differential charge density $\rho_{\mathrm{electron}}(\vec{r}) - \rho_{\mathrm{atom}}(\vec{r})$, where the electron redistribution highlights the interfacial hydrogen-bonding network. Water molecules in the first and second wetting layers having representative configurations of the distributions in Figs. 2a-2c are circled by black and dashed red lines, respectively

B. Effect of low NaCl salinity

The carbonate reservoir is initially in equilibrium with formation water, which contains a high concentration of NaCl. In a previous DFT study, the low-salinity effect was considered in terms of the dielectric constant variation in the continuum solvent model[33]. Here we consider the incorporation of Na^+ and Cl^- ions in the brine explicitly. With the addition of NaCl salt, a typical double layer is formed in the vicinity of the calcite surface, as shown in Fig. 3a. It is worth pointing out that the presence of a double layer does not necessarily require the surface to be charged[28]. As already demonstrated, the calcite surface is strongly hydrophilic, i.e. water molecules in the first two wetting layers are strongly adsorbed to the calcite surface. We find that Na^+ and Cl^- ions are unable to penetrate the first two wetting layers, due to the large energy penalty that needs to be paid for reconstructing the interfacial hydrogen-bonding network.

Besides, Na^+ ions sit closer to the calcite surface than Cl^- ions, possibly due to the smaller ionic radius of Na^+ ions.

However, Na^+ and Cl^- ions establish their solvation shells, which interact with the calcite surface through the hydrogen-bonding network in the first two wetting layers. Upon the "proximal adsorption" of Na^+ and Cl^- ions, the first wetting layer slightly depletes from the calcite surface (Fig. 3a, highlighted by the comparison between black and grey lines). As a result, interfacial water structure (especially the orientation angle and O-H bond angle distributions) is significantly modified, as shown in Fig. 3c-3d. This result strongly indicates that the adhesion between the calcite surface and the NaCl brine becomes weaker, resulting in a less water-wet (more oil-wet) state.

Indeed, assuming an initial mixed-wet state ($\theta_0 = 90°$), the calcite surface is driven to the oil-wet state by 24° upon wetted by 0.6 M NaCl brine, as shown in Fig. 1c. This result manifests the low-salinity effect that is observed in many experiments[14-16,18,19], and is in line with a recent contact angle measurement[18] (more oil-wet by 50° upon wetted by 1.0 M NaCl brine). It is worth noting that, in experiments, non-monotonicity of the dependence of contact angle on NaCl concentration was found[18], i.e. with increasing the NaCl concentration the calcite surface became firstly more water-wet at 0.001 M. Unfortunately, we are unable to verify this non-monotonicity, since such low concentration is unreachable by quantum MD simulations.

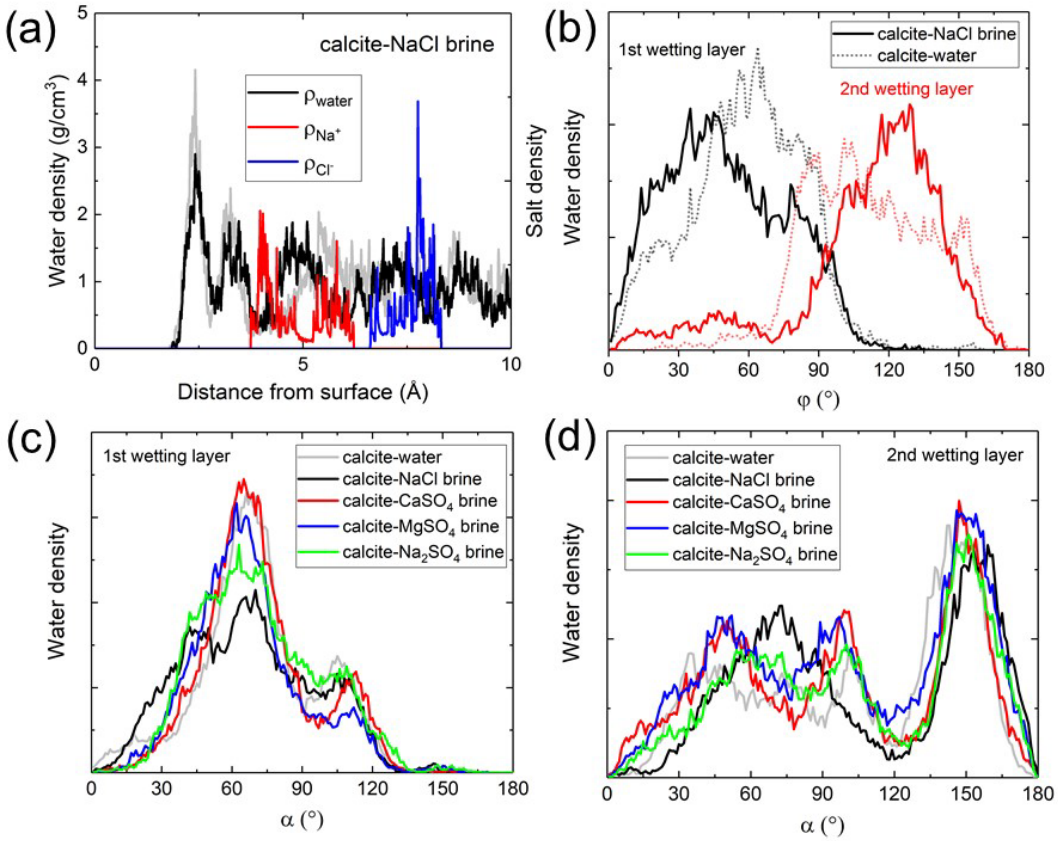

Figure 3. (a) For calcite-NaCl brine: density profiles of water and NaCl salt ions along the surface normal. The water density profile for calcite-water is shown by the grey line for comparison. (b) For calcite-NaCl brine: orientation angle distribution of water molecules in the first wetting layer, compared to calcite-water. (c, d) O-H bond angle distribution of water molecules in the first and second wetting layers.

C. Effect of potential determining ions Ca^{2+}, Mg^{2+}, and SO_4^{2-}

In the above discussions, we have demonstrated that the low-salinity effect originates from the fundamental role of Na^+ ions as the "interfacial water structure breaker". This is not the case for calcite-$CaSO_4$/$MgSO_4$ brine. The proximal adsorption of Ca^{2+}, Mg^{2+}, and SO_4^{2-} ions also occurs above the first two wetting layers, with the metal cations Ca^{2+}/Mg^{2+} sitting closer to the surface than anions SO_4^{2-}, as shown in Fig. 4a. The interfacial water structure, however, is hardly modified, as shown in Fig. 3c-3d. This result is possibly due to the fact that divalent Ca^{2+} and Mg^{2+} ions sit slightly farther away from the calcite surface than monovalent Na^+ ions (see Figs. 3a and 4a).

In fact, in many laboratory investigations, Ca^{2+}, Mg^{2+}, and SO_4^{2-} ions present in seawater are often described as "potential determining ions" as they have great impact on the surface charge[9-13]. The initial (positive or negative) surface charge might depend on the experimental conditions[9-13]. We find that the water-wetted calcite surface is "positively charged" by 0.103 e per surface $CaCO_3$ unit (estimated from Mulliken population analysis). While the laboratory observation of the positive surface charge results possibly from surface complexation of ions[68,69], the present calculations provide an indication of an intrinsic effective surface charge on the calcite surface induced by the ions. Besides, zeta potential measurements showed that adsorption of metal ions Ca^{2+} and Mg^{2+} raises the surface charge while adsorption of SO_4^{2-} ions lowers the surface charge[13]. It has been further suggested that adsorption of sulfate ions facilitates the desorption of the negatively charged carboxylic group due to the electrostatic interaction[9-13].

Due to the electronic redistribution induced by the proximal adsorption of Ca^{2+}, Mg^{2+}, and SO_4^{2-} ions, the calcite surface becomes more positively charged, as shown in Fig. 1c. The enhanced "charge transfer" (from the calcite surface to brine) results in stronger electrostatic interactions between the calcite surface and the interfacial water, and hence stronger hydrophilicity. Indeed, the calcite surface becomes more water-wet when wetted by 0.3 M $CaSO_4$/$MgSO_4$ brine, as shown in Fig. 1c. Such "charge transfer" is more pronounced for Ca^{2+} ions than Mg^{2+} ions, indicating that Ca^{2+} ions are more effective wettability modifiers. One could also see from Fig. 1c that the proximal adsorption of Na^+ and Cl^- ions hardly induce any charge transfer. These findings are in line with experimental observations[9-13] that Ca^{2+}, Mg^{2+}, and SO_4^{2-} ions are "potential determining".

To further illustrate specifically the role of SO_4^{2-} ions, we study calcite-Na_2SO_4 brine where Na^+ and SO_4^{2-} ions compete with each other. On one hand, the interfacial water structure is slightly modified, possibly due to the reminiscent effect of Na^+ ions as interfacial water structure

breakers, as shown in Fig. 3c-3d. On the other hand, charge transfer occurs, as shown in Fig. 1c. The net effect is to render the calcite surface more water-wet, as shown in Fig. 1c. In fact, the calcite-Na_2SO_4 brine wettability is only slightly less water-wet than calcite-$CaSO_4$ brine.

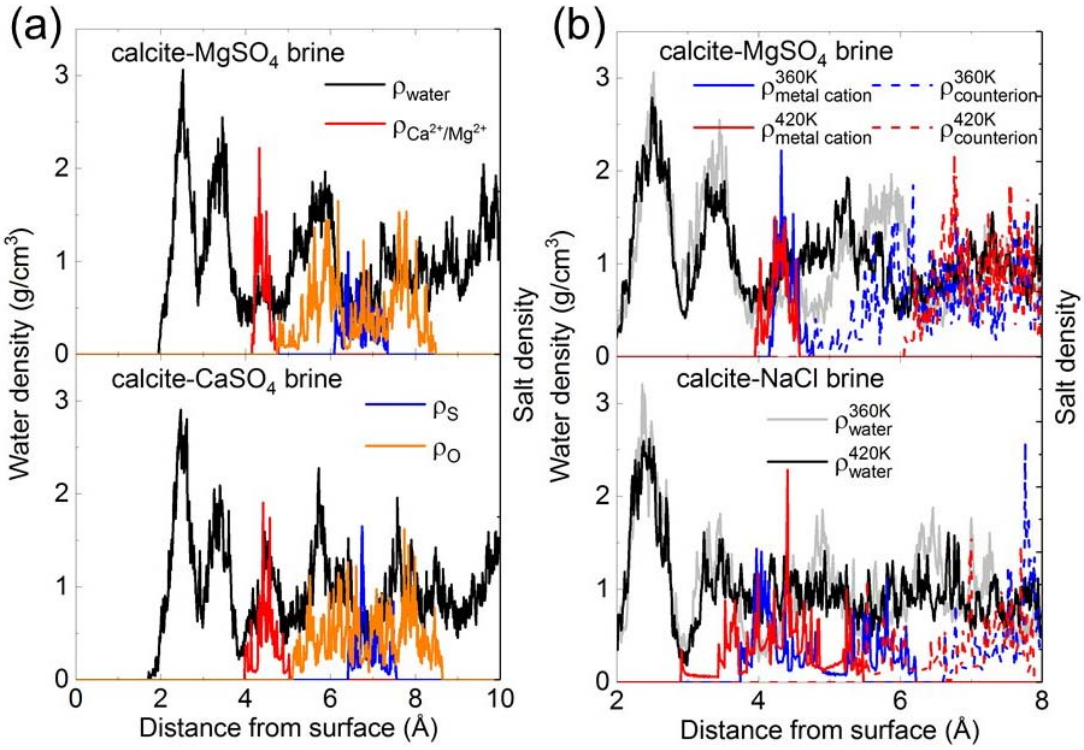

Figure 4. (a) Density profiles of water and $CaSO_4$/$MgSO_4$ salt ions along the surface normal. (b) Density profiles of water and $MgSO_4$/NaCl salt ions along the surface normal at different temperatures.

D. Effect of temperature

The positive impact of temperature (the carbonate reservoir becomes more water-wet with increasing the temperature) has been reported in experiments[10,12,14]. For potential determining ions, it was attributed to the more pronounced surface charge alteration, as ion adsorption was enhanced by increasing the temperature[5, 7]. The present calculations partly support such suggested mechanism. As shown in the upper panel of Fig. 4b, for the case of calcite-$MgSO_4$, the metal cation Mg^{2+} sits closer to the surface with increasing temperature. However, contrary to the general expectation that the co-adsorption of SO_4^{2-} would be facilitated, we find that SO_4^{2-} is driven further away from the calcite surface. As a result, the calcite surface becomes even more positively charged. Assuming a correlation between wettability alteration and interfacial charge transfer for potential determining ions, the calcite surface hence becomes more water-wet. This finding provides an alternative insight for the role of Mg^{2+} ions as wettability modifiers at high temperatures, in addition to the substitution mechanism[12,32].

In the low-salinity effect, the positive impact of temperature is also manifested. For calcite-NaCl brine, with increasing the temperature, while the first two wetting layers are still present, the

proximal adsorption of Na^+ and Cl^- ions occurs closer to the calcite surface, as shown in the lower panel of Fig. 4b. More importantly, at high temperatures, Na^+ ions even become capable of penetrating the second wetting layer, and therefore the impact of disrupting the interfacial water structure is enhanced.

E. Core-flooding experiments

We have demonstrated with simulations that with the dilution of NaCl salinity and addition of Ca^{2+}, Mg^{2+} and SO_4^{2-} ions, the calcite surface becomes more water-wet and hence EOR is expected. To further corroborate such results, we performed core-flooding experiments on a carbonate core saturated with ADNOC crude oil with different brines: formation water (FW), 4-times diluted seawater (4dSW) and 4-times diluted seawater with the addition of 3-times sulfates (4dSW3S). As shown in Fig. 5a, the recovery from FW is 51%. Oil recovery is enhanced by 15% when the injected seawater is 4-times diluted. With the addition of 3-times sulfates, oil recovery is further enhanced by 14%. Our core flooding measurements are hence in line with quantum MD simulations.

To further investigate if the presence of Ca^{2+} ions is required for SO_4^{2-} ions to alter the wettability, we removed Ca^{2+} ions from 4dSW3S (referred to as 4dSW3S0Ca), and performed comparative spontaneous imbibition experiments with the two brines having the same ionic strength. The experiments were performed on cores that were saturated with ADNOC crude oil. During the imbibition, dissolution of the calcite surface takes place until an equilibrium of Ca^{2+} concentration is achieved. However, similar oil recovery is observed for the two brines over time. As shown in Fig. 5b, the recovery from 4dSW3S is 20.8% whereas the recovery from 4dSW3S0Ca is 22.6%, suggesting SO_4^{2-} rather than Ca^{2+} ions as wettability modifiers. This result is again in line with quantum MD simulations.

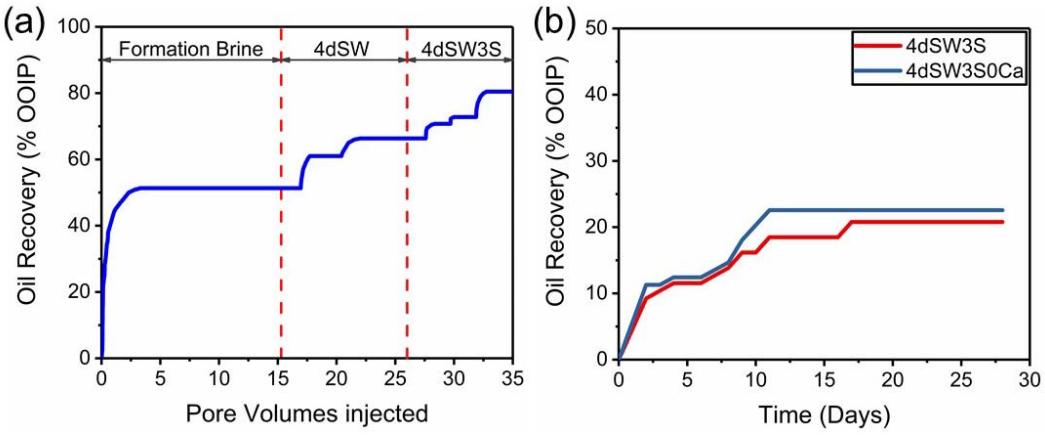

Figure 5. (a) Core flooding recovery results with three brines (see text): FW, 4dSW, and 4dSW3S. (b) Spontaneous imbibition experiments with two brines (see text): 4dSW3S and 4dSW3S0Ca.

IV. CONCLUSIONS

In conclusion, we have performed extensive quantum MD simulations to study the wettability alteration mechanism responsible for EOR at the calcite-brine interface. Wettability is reliably characterized by the contact angle using the work-of-adhesion approach. Complete water wetting is predicted for calcite surfaces with strongly hydrophilic first two wetting layers that hinder wettability modifiers (Na^+, Cl^-, Ca^{2+}, Mg^{2+}, and SO_4^{2-} ions) from reaching the surface. The impact of such proximal adsorption on wettability alteration is two-fold: Na^+ and Cl^- ions settle closer to the surface, disturbing the interfacial water structure and rendering the calcite surface less water-wet (which inhibits oil recovery), while Ca^{2+}, Mg^{2+} and SO_4^{2-} ions settle farther from the surface, modifying the surface charge and rendering the calcite surface more water-wet (which enhances oil recovery). The impact is more pronounced at high temperatures as the proximal adsorption is enhanced. Our core-flooding and spontaneous imbibition experiments corroborate the theoretical results and further demonstrate the role of SO_4^{2-} rather than Ca^{2+} ions as wettability modifiers. The present study opens the avenue to study the wettability alteration mechanism at the atomic scale, and brings physical insights into the underlying role of wettability modifiers. For the purpose of EOR, the following characteristics are desired in designing smart water: low NaCl concentration, high $CaSO_4$/$MgSO_4$ concentration, and high temperature.

Acknowledgements

This work was supported in part by the Abu Dhabi National Oil Company (ADNOC) and by the McMinn Endowment at Vanderbilt University. Computations were carried out at the National Energy Research Scientific Computing Center, a DOE Office of Science User Facility supported by the Office of Science of the U.S. Department of Energy under Contract No. DE-AC02-05CH11231, and the Extreme Science and Engineering Discovery Environment (XSEDE), which is supported by National Science Foundation grant number ACI-1053575.

[1] N. Shenogina, R. Godawat, P. Keblinski and S. Garde, How wetting and adhesion affect thermal conductance of a range of hydrophobic to hydrophilic aqueous interfaces, Phys. Rev. Lett. **102**, 156101 (2009).

[2] C. Zhu, H. Li, Y. Huang, X. Zeng and S. Meng, Microscopic insight into surface wetting: Relations between interfacial water structure and the underlying lattice constant, Phys. Rev. Lett. **110**, 126101 (2013).

[3] P. Guo, Y. Tu, J. Yang, C. Wang, N. Sheng and H. Fang, Water-COOH composite structure with enhanced hydrophobicity formed by water molecules embedded into carboxyl-terminated self-assembled monolayers, Phys. Rev. Lett. **115**, 186101 (2015).

[4] B. Fan, F. Li, L. Chen, L. Shi, W. Yan, Y. Zhang, S. Li, X. Wang, X. Wang and H. Chen, Photovoltaic manipulation of water microdroplets on a hydrophobic $LiNbO_3$ substrate, Phys. Rev. Appl. **7**, 064010 (2017).

[5] P. C. Myint and A. Firoozabadi, Thin liquid films in improved oil recovery from low-salinity brine, Curr. Opin. Colloid Interface Sci. **20**, 105 (2015).

[6] A. RezaeiDoust, T. Puntervold, S. Strand and T. Austad, Smart water as wettability modifier in carbonate and sandstone: A discussion of similarities/differences in the chemical mechanisms, Energy Fuels **23**, 4479 (2009).

[7] J. Song, Y. Zeng, L. Wang, X. Duan, M. Puerto, W. G. Chapman, S. L. Biswal and G. J. Hirasaki, Surface complexation modeling of calcite zeta potential measurements in brines with mixed potential determining ions (Ca^{2+}, $CO3^{2-}$, Mg^{2+}, $SO4^{2-}$) for characterizing carbonate wettability, J. Colloid Interface Sci. **506**, 169 (2017).
[8] M. A. Sohal, G. Thyne and E. G. Søgaard, Review of recovery mechanisms of ionically modified waterflood in carbonate reservoirs, Energy Fuels **30**, 1904 (2016).
[9] P. Zhang, M. T. Tweheyo and T. Austad, Wettability alteration and improved oil recovery in chalk: The effect of calcium in the presence of sulfate, Energy Fuels **20**, 2056 (2006).
[10] S. Strand, E. J. Høgnesen and T. Austad, Wettability alteration of carbonates - Effects of potential determining ions (Ca^{2+} and $SO4^{2-}$) and temperature, Colloids Surf. A Physicochem. Eng. Asp. **275**, 1 (2006).
[11] P. Zhang and T. Austad, Wettability and oil recovery from carbonates: Effects of temperature and potential determining ions, Colloids Surf. A Physicochem. Eng. Asp. **279**, 179 (2006).
[12] P. Zhang, M. T. Tweheyo and T. Austad, Wettability alteration and improved oil recovery by spontaneous imbibition of seawater into chalk: Impact of the potential determining ions Ca^{2+}, Mg^{2+}, and $SO4^{2-}$, Colloids Surf. A Physicochem. Eng. Asp. **301**, 199 (2007).
[13] A. Kasha, H. Al-Hashim, W. Abdallah, R. Taherian and B. Sauerer, Effect of Ca^{2+}, Mg^{2+} and $SO4^{2-}$ ions on the zeta potential of calcite and dolomite particles aged with stearic acid, Colloids Surf. A Physicochem. Eng. Asp. **482**, 290 (2015).
[14] Y. Lu, N. F. Najafabadi and A. Firoozabadi, Effect of temperature on wettability of oil/brine/rock systems, Energy Fuels **31**, 4989 (2017).
[15] A. A. Yousef, S. H. Al-Saleh, A. Al-Kaabi and M. S. Al-Jawfi, Laboratory investigation of the impact of injection-water salinity and ionic content on oil recovery from carbonate reservoirs, SPE Reserv. Eval. Eng. **14**, 578 (2011).
[16] S. J. Fathi, T. Austad and S. Strand, Water-based enhanced oil recovery (EOR) by "smart water": Optimal ionic composition for EOR in carbonates, Energy Fuels **25**, 5173 (2011).
[17] M. Trojer, M. L. Szulczewski and R. Juanes, Stabilizing fluid-fluid displacements in porous media through wettability alteration, Phys. Rev. Appl. **3**, 054008 (2015).
[18] S. Aslan, N. Fathi Najafabadi and A. Firoozabadi, Non-monotonicity of the contact angle from NaCl and $MgCl_2$ concentrations in two petroleum fluids on atomistically smooth surfaces, Energy Fuels **30**, 2858 (2016).
[19] A. A. Yousef, S. Al-Saleh and M. S. Al-Jawfi, in *SPE Improved Oil Recovery Symposium* (Society of Petroleum Engineers, 2012).
[20] S.-Y. Chen, Y. Kaufman, K. Kristiansen, D. Seo, A. M. Schrader, M. B. Alotaibi, H. A. Dobbs, N. A. Cadirov, J. R. Boles and S. C. Ayirala, Effects of salinity on oil recovery (the "dilution effect"): Experimental and theoretical studies of crude oil/brine/carbonate surface restructuring and associated physicochemical interactions, Energy Fuels **31**, 8925 (2017).
[21] H. Mahani, A. L. Keya, S. Berg, W.-B. Bartels, R. Nasralla and W. R. Rossen, Insights into the mechanism of wettability alteration by low-salinity flooding (LSF) in carbonates, Energy Fuels **29**, 1352 (2015).
[22] B. J. Chun, S. G. Lee, J. I. Choi and S. S. Jang, Adsorption of carboxylate on calcium carbonate surface: Molecular simulation approach, Colloids Surf. A Physicochem. Eng. Asp. **474**, 9 (2015).
[23] G. Lu, X. Zhang, C. Shao and H. Yang, Molecular dynamics simulation of adsorption of an oil-water-surfactant mixture on calcite surface, Pet. Sci. **6**, 76 (2009).
[24] M. H. Ghatee, M. M. Koleini and S. Ayatollahi, Molecular dynamics simulation investigation of hexanoic acid adsorption onto calcite surface, Fluid Ph. Equilibria **387**, 24 (2015).
[25] N. Bovet, M. Yang, M. S. Javadi and S. L. S. Stipp, Interaction of alcohols with the calcite surface, Phys. Chem. Chem. Phys. **17**, 3490 (2015).

[26] S. Yuan, S. Wang, X. Wang, M. Guo, Y. Wang and D. Wang, Molecular dynamics simulation of oil detachment from calcite surface in aqueous surfactant solution, Comput. Theor. Chem. **1092**, 82 (2016).
[27] X. Chang, Q. Xue, X. Li, J. Zhang, L. Zhu, D. He, H. Zheng, S. Lu and Z. Liu, Inherent wettability of different rock surfaces at nanoscale: a theoretical study, Appl. Surf. Sci. **434**, 73 (2018).
[28] D. Spagnoli, D. J. Cooke, S. Kerisit and S. C. Parker, Molecular dynamics simulations of the interaction between the surfaces of polar solids and aqueous solutions, J. Mater. Chem. **16**, 1997 (2006).
[29] M. Ricci, P. Spijker, F. Stellacci, J.-F. Molinari and K. Voïtchovsky, Direct visualization of single ions in the Stern layer of calcite, Langmuir **29**, 2207 (2013).
[30] H. Chen, A. Z. Panagiotopoulos and E. P. Giannelis, Atomistic molecular dynamics simulations of carbohydrate–calcite interactions in concentrated brine, Langmuir **31**, 2407 (2015).
[31] M. M. Koleini, M. F. Mehraban and S. Ayatollahi, Effects of low salinity water on calcite/brine interface: A molecular dynamics simulation study, Colloids Surf. A **537**, 61 (2018).
[32] H. Sakuma, M. P. Andersson, K. Bechgaard and S. L. S. Stipp, Surface tension alteration on calcite, induced by ion substitution, J. Phys. Chem. C **118**, 3078 (2014).
[33] V. M. Sánchez and C. R. Miranda, Modeling acid oil component interactions with carbonate reservoirs: a first-principles view on low salinity recovery mechanisms, J. Phys. Chem. C **118**, 19180 (2014).
[34] M. P. Andersson, K. Dideriksen, H. Sakuma and S. L. S. Stipp, Modelling how incorporation of divalent cations affects calcite wettability–implications for biomineralisation and oil recovery, Sci. Rep. **6**, 28854 (2016).
[35] M. P. Andersson, H. Sakuma and S. L. S. Stipp, Strontium, nickel, cadmium, and lead substitution into calcite, studied by density functional theory, Langmuir **30**, 6129 (2014).
[36] D. Addari and A. Satta, Influence of HCOO- on calcite growth from first-principles, J. Phys. Chem. C **119**, 19780 (2015).
[37] S. T. Pantelides, S. Prabhakar, J. Liu, Y.-Y. Zhang, C.-Y. Lai, M. Chiesa and S. Alhassan, in *SPE Abu Dhabi International Petroleum Exhibition & Conference* (Society of Petroleum Engineers, 2017).
[38] J. Y. Lu, Q. Ge, H. Li, A. Raza and T. Zhang, Direct prediction of calcite surface wettability with first-principles quantum simulation, J. Phys. Chem. Lett. **8**, 5309 (2017).
[39] B. Ramos-Alvarado, S. Kumar and G. P. Peterson, Wettability of graphitic-carbon and silicon surfaces: MD modeling and theoretical analysis, J. Chem. Phys. **143**, 044703 (2015).
[40] F. Taherian, V. Marcon, N. F. A. van der Vegt and F. Leroy, What is the contact angle of water on graphene?, Langmuir **29**, 1457 (2013).
[41] F. Leroy, S. Liu and J. Zhang, Parametrizing nonbonded interactions from wetting experiments via the work of adhesion: Example of water on graphene surfaces, J. Phys. Chem. C **119**, 28470 (2015).
[42] V. Kumar and J. R. Errington, Wetting behavior of water near nonpolar surfaces, J. Phys. Chem. C **117**, 23017 (2013).
[43] F. Taherian, F. d. r. Leroy and N. F. van der Vegt, Interfacial entropy of water on rigid hydrophobic surfaces, Langmuir **29**, 9807 (2013).
[44] J. Liu, C.-Y. Lai, Y.-Y. Zhang, M. Chiesa and S. T. Pantelides, Water wettability of graphene: interplay between the interfacial water structure and the electronic structure, RSC Advances **8**, 16918 (2018).
[45] J. Liu and S. T. Pantelides, Electrowetting on two-dimensional dielectrics: a quantum molecular dynamics investigation., J. Phys.: Condens. Matter **30**, 375001 (2018).
[46] R. G. Mortimer, *Physical chemistry* (Elsevier Academic Press, 2008).
[47] R. Shuttleworth, The surface tension of solids, Proc. Phys. Soc., Sec. A **63**, 444 (1950).
[48] N. Vargaftik, B. Volkov and L. Voljak, International tables of the surface tension of water, J. Phys. Chem. Ref. Data **12**, 817 (1983).

[49] D. Okhrimenko, J. Nissenbaum, M. P. Andersson, M. H. M. Olsson and S. L. S. Stipp, Energies of the adsorption of functional groups to calcium carbonate polymorphs: the importance of -OH and -COOH groups, Langmuir **29**, 11062 (2013).
[50] D. J. Cooke, R. J. Gray, K. K. Sand, S. L. S. Stipp and J. Elliott, Interaction of ethanol and water with the {1014} surface of calcite, Langmuir **26**, 14520 (2010).
[51] H. N. Sørgård, C. Totland, W. Nerdal and J. G. Seland, Crude oil adsorbates on calcite and quartz surfaces investigated by NMR spectroscopy, J. Phys. Chem. C **121**, 20892 (2017).
[52] D. Surblys, F. Leroy, Y. Yamaguchi and F. Müller-Plathe, Molecular dynamics analysis of the influence of Coulomb and van der Waals interactions on the work of adhesion at the solid-liquid interface, J. Chem. Phys. **148**, 134707 (2018).
[53] J. M. Soler, E. Artacho, J. D. Gale, A. García, J. Junquera, P. Ordejón and D. Sánchez-Portal, The SIESTA method for ab initio order-N materials simulation, J. Phys.: Condens. Matter **14**, 2745 (2002).
[54] M. Fernández-Serra and E. Artacho, Network equilibration and first-principles liquid water, J. Chem. Phys. **121**, 11136 (2004).
[55] J. Wang, G. Román-Pérez, J. M. Soler, E. Artacho and M.-V. Fernández-Serra, Density, structure, and dynamics of water: The effect of van der Waals interactions, J. Chem. Phys. **134**, 024516 (2011).
[56] S. Y. Willow, X. C. Zeng, S. S. Xantheas, K. S. Kim and S. Hirata, Why is MP2-water "cooler" and "eenser" than DFT-water?, J. Phys. Chem. Lett. **7**, 680 (2016).
[57] M. M. Szcz□śniak and S. Scheiner, Correction of the basis set superposition error in SCF and MP2 interaction energies. The water dimer, J. Chem. Phys. **84**, 6328 (1986).
[58] R. S. Mulliken, Electronic population analysis on LCAO–MO molecular wave functions. I, J. Chem. Phys. **23**, 1833 (1955).
[59] K. Nayar, D. Panchanathan, G. McKinley and J. Lienhard, Surface tension of seawater, J. Phys. Chem. Ref. Data **43**, 043103 (2014).
[60] S. Zeppieri, J. Rodríguez and A. López de Ramos, Interfacial tension of alkane + water systems, J. Chem. Eng. Data **46**, 1086 (2001).
[61] E. Lima, B. De Melo, L. Baptista and M. Paredes, Specific ion effects on the interfacial tension of water/hydrocarbon systems, Braz. J. Chem. Eng. **30**, 55 (2013).
[62] A. Kakati and J. S. Sangwai, Effect of monovalent and divalent salts on the interfacial tension of pure hydrocarbon-brine systems relevant for low salinity water flooding, J. Petrol. Sci. Eng. **157**, 1106 (2017).
[63] S. Kerisit and S. C. Parker, Free energy of adsorption of water and metal ions on the {1014} calcite surface, J. Am. Chem. Soc. **126**, 10152 (2004).
[64] P. Fenter and N. Sturchio, Calcite (104)–water interface structure, revisited, Geochim. Cosmochim. Acta **97**, 58 (2012).
[65] D. K. Owens and R. Wendt, Estimation of the surface free energy of polymers, J. Appl. Polym. Sci. **13**, 1741 (1969).
[66] D. Y. Kwok and A. W. Neumann, Contact angle measurement and contact angle interpretation, Adv. Colloid Interface Sci. **81**, 167 (1999).
[67] C.-Y. Lai, M. Cozzolino, M. V. Diamanti, S. Al Hassan and M. Chiesa, Underlying mechanism of time dependent surface properties of calcite ($CaCO_3$): A baseline for investigations of reservoirs wettability, J. Phys. Chem. C **119**, 29038 (2015).
[68] P. Van Cappellen, L. Charlet, W. Stumm and P. Wersin, A surface complexation model of the carbonate mineral-aqueous solution interface, Geochim. Cosmochim. Acta **57**, 3505 (1993).
[69] P. V. Brady and G. Thyne, Functional wettability in carbonate reservoirs, Energy Fuels **30**, 9217 (2016).